Embedded Optical Waveguide Sensors for Dynamic Behavior Monitoring in Twisted-Beam Structures

Paul Bupe, Jr.¹, Yuhao Jiang², J-T. Lin¹, Tram Nguyen¹, Michael S. Han¹, Daniel M. Aukes², C. K. Harnett¹

Abstract—In this work, we present two embedded soft optical waveguide sensors designed for real-time onboard configuration sensing in soft actuators for robotic locomotion. Extending the contributions of our collaborators who employed external camera systems to monitor the gaits of twisted-beam structures, we strategically integrate our OptiGap sensor system into these structures to monitor their dynamic behavior. The system is validated through machine learning models that correlate sensor data with camera-based motion tracking, achieving high accuracy in predicting forward or reverse gaits and validating its capability for real-time sensing. Our second sensor, consisting of a square cross-section fiber pre-twisted to 360 degrees, is designed to detect the chirality of reconfigurable twisted beams. Experimental results confirm the sensor's effectiveness in capturing variations in light transmittance corresponding to twist angle, serving as a reliable chirality sensor. The successful integration of these sensors not only improves the adaptability of soft robotic systems but also opens avenues for advanced control algorithms.

I. INTRODUCTION

Soft robots need onboard configuration sensing that doesn't affect their overall mechanics. Mechanical transparency is especially important in cases where the robot's function depends closely on its material properties. The first application we explore in this paper (Fig. 1a) is a twisted soft beam developed by our collaborators [1] that achieves walking gaits at specific frequencies when vibrated by a single-direction excitation. Gaits, however, depend on beam loading, surface contact, and properties of the surrounding environment such as viscosity and density - all of which may change during run time. The second application we explore in this paper are optically-sensed beams (Fig. 1b) having reconfigurable left-handed or right-handed twist direction. In the case of these reconfigurable twisted beams, feedback is needed to verify that reconfiguration is complete. To monitor the real-time dynamics (as in the first application) and the static chirality (in the second application), sensors should be small or at least unobtrusive enough that they don't interfere with motions. With self-sensing capability, these robots will gain the ability to adapt to surroundings, for example changing frequency when swimming in media with varying density or flow velocity, and detecting collisions

This work is supported by the National Science Foundation [NSF Award #1935324]

Corresponding author: C. K. Harnett (e-mail: c0harn01@louisville.edu)

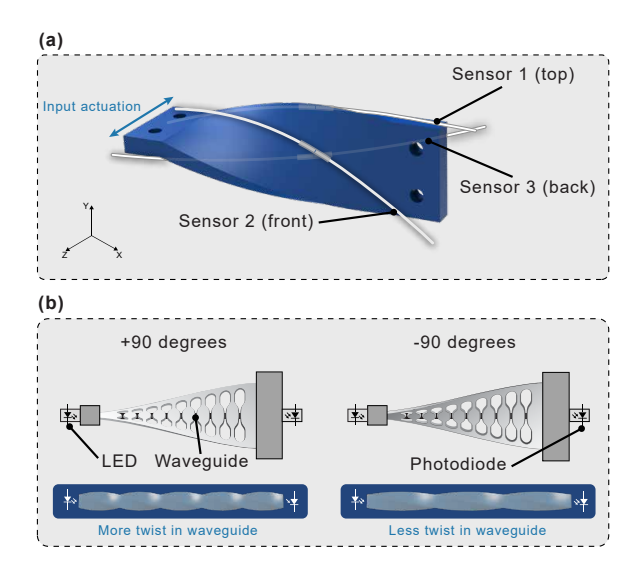


Fig. 1. **Experimental setups.** (a) Positions of the 3 OptiGap sensors. Sensors 2 and 3 intersect in the middle on each side of the beam while sensor 1 is placed along the top edge. (b) Overview of the chirality sensor. The square fiber is initially pretwisted to 360 degrees which results in less twist once the twisted beam rotates.

with objects. In both applications, the embedded sensors need to report on motions at frequencies up to 100 Hz in real time. In terms of specific needs for the materials, their elastic properties should be similar to those of soft robotics materials such as thermoplastic urethane (TPU) and silicone; they should function in wet environments; they should be sensitive to specific modes of deformation (bending, twisting) at specific locations; they should also be immune to the effects of temperature and drift, a common issue found with traditional strain sensors. The OptiGap sensor system [2] we recently introduced meets all these requirements for use in these applications, which are part of a new class of soft robots called Soft, Curved, Reconfigurable, Anisotropic Mechanisms, or SCRAMs [1]–[7].

A. Machine Learning Techniques

In the first application, we focus on the twisted soft beam's real-time dynamics. To capture these dynamics, three OptiGap sensors are strategically placed (Fig. 1a) on the beam: one along the top edge, another across the front, and the third across the back face at a 90-degree angle to the front sensor. These placements are designed to capture the beam's vibrational characteristics as it interacts with its

¹ Speed School of Engineering, University of Louisville, Louisville, KY, 40292 USA

² The School for Manufacturing Systems and Networks, Fulton Schools of Engineering, Arizona State University, Mesa, AZ, 85212, USA

environment. As the beam vibrates within the $1\,\mathrm{Hz}$ to $45\,\mathrm{Hz}$ range, the sensors record optical intensity data, which is then correlated with position data of the beam's tip captured by a precise motion tracking system. This dataset, comprising x, y, z tip positions and optical intensity readings from the three sensors, serves as the foundation for our machine learning approach. By training machine learning models on this data, we aim to predict the direction of the beam's motion (forward or backward) at its point of contact, offering a unique method for real-time bend sensing in flexible structures. Our collaborators determine the direction of motion using a commercial camera-based motion tracking system as well as direct observation on a test platform.

Machine learning techniques have become important in the classification of real-time sensor data across many domains [8]–[13]. Tan et al. [8] introduce a modified Long Short-Term Memory (LSTM) network for detecting heel strikes and toe offs in gait cycles. When tested against the Movement Analysis in Real-world Environments using Accelerometers (MAREA) database, this method shows improved results compared to six other gait event detection algorithms. Other techniques include Vu et al.'s development of the Exponentially Delayed Fully Connected Neural Network (ED-FNN) for gait cycle percentage prediction [9], Khandelwal et al.'s DK-TiFA methodology for Initial Contact event estimation from accelerometers [10], and Su et al.'s use of the Deep Convolutional Neural Network (DCNN) for gait cycle segmentation with IMU data [12].

Logistic regression and random forest are both popular machine learning algorithms used for binary classification tasks due to their simplicity when compared to the aforementioned neural network approaches. Logistic regression is a linear model that estimates the probability of a binary outcome based on one or more predictor variables [14]. On the other hand, random forest is an ensemble learning method that constructs multiple decision trees during training and outputs the mode of the classes (classification) of the individual trees for prediction. It effectively addresses the overfitting problem seen in individual decision trees by averaging out biases and capturing the underlying patterns in the data [15]. While logistic regression assumes a linear relationship between predictors and the log odds of the outcome, random forest makes no such assumption, allowing it to capture complex, non-linear relationships in the data. Bahel et al. in [16] provide a comparison of binary classification algorithms, highlighting the extreme effectiveness of the random forest classifier.

B. Embedded Optical Sensing

In the second application, the focus shifts to directly sensing the chirality of a reconfigurable twisted beam, an important factor affecting the trajectory of the beam's endpoint. Inspired by natural examples such as twisting animal muscles [17] and shape-morphing plant seeds [18], researchers have developed reconfigurable twisting beams with applications in robotic manipulation and locomotion. Driving methods include cables [19] and inflatable chambers [17], liquid

crystal elastomers [20], and shape memory alloy wires [21]. In these works, the focus is on inducing and controlling twist rather than self shape-sensing, and bistable examples are scarce. In [22], a carbon fiber composite beam is given bistable twisting states by inserting strain. Pre-curved strips are straightened for attachment to the edges of the beam. The stored strain energy is relieved when the beam twists in either a left- or right-handed direction, with transitions over an 80 degree range demonstrated using piezoelectric actuators. In the present work, however, a 180 degree transition range is required and the materials must be soft enough to match the properties of the 3D printed fixed-twist structures. These requirements are met by using axial tension to create twist in a thin polycarbonate skeleton that can compress along the center but not along its edges, and the tension spring provides a path for an embedded optical twist sensor.

Recent advancements in soft robotics emphasize the integration of such soft sensors to improve real-time feedback and adaptability [23]-[30]. Al Jaber et al. [28] introduce a method for registering the shape and orientation of soft robots using segmented optical fibers, a camera, and a calibration algorithm, demonstrating its potential for accurate shape reconstruction of continuum soft robots. Another work [23] presents stretchable optical waveguides as strain sensors for prosthetics, underscoring their potential in improving sensory capabilities in soft robotic systems. Next, Galloway et al. [30] integrates a fiber optic shape sensor into soft robotic systems, offering high-resolution shape information, while Every et al. [27] introduces a proprioceptive soft actuator using electrical impedance tomography for shape sensing. A roughness tuning strategy for fabricating multi-modal soft optical sensors is also presented [25], emphasizing their utility in soft robot controllability. Finally, [24], [26], [31] further explore optical, electro-conductive yarn, and piezoelectric sensing mechanisms, respectively, in applications ranging from wearable sensing technologies to minimally invasive surgery. These works underscore the the importance of real-time soft sensing for feedback and adaptability.

In this application, a soft optical sensor is developed, shown in Fig. 1b, that uses a pre-twisted square cross-section silicone fiber (waveguide) threaded through a tube along the central axis of a beam. The transmittance of this waveguide has an inverse relationship to the amount of twist in the waveguide, which can be used to sense the chirality of the beam. This sensing capability is especially useful in bistable twisted structures where the same limb can produce different foot motions (e.g. forward vs backwards) depending on its chirality when oscillated at a constant frequency. This sensor's broader applications can extend to monitoring device configuration during reconfiguration and detecting unintended chirality shifts during high-amplitude motions or collisions, highlighting its role in improving real-time feedback and adaptability in soft robotic systems.

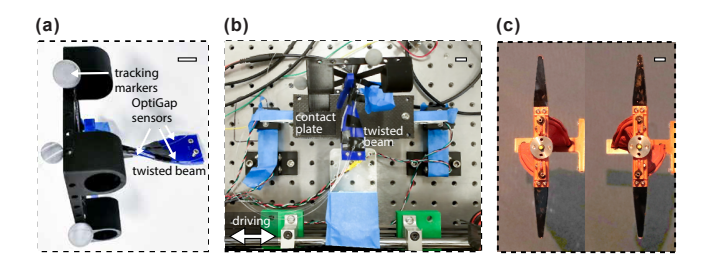


Fig. 2. Photographs of (a,b) vibrating beam with sensors using the same test setup from [1] showing the translational stage, rigid foot, optical tracking markers, and 50 g mass, and (c) reconfigurable twisted beam in its two stable states. Scale bars are 1 cm.

II. MATERIALS AND METHODS

A. Determining Contact Direction

1) Real-time Classification: The first application employs 500 um Polymethyl methacrylate (PMMA) optical fiber sensors integrated into the OptiGap system. Three fibers, featuring small air gaps enclosed by a flexible sleeve as core sensing elements, are strategically placed on the surface of the twisted soft beam. As first introduced [2], the OptiGap system uses these air gaps in flexible optical light pipes to create coded segments for bend localization, but in this application, the OptiGap system captures dynamic behavior and vibrations in the beam, particularly when oscillated horizontally at frequencies ranging from 1 Hz to 40 Hz.

The main objective is to construct a real-time binary classification model capable of determining the direction of motion at the point of contact (with the two classes being "forward" and "backward") for the beam, utilizing data from the three OptiGap sensors. Logistic regression (LR) serves as the baseline model, providing a straightforward yet effective starting point for classification. This is followed by the implementation of a random forest (RF) model, which offers a more effective approach to capturing complex data patterns. Given the sequential nature of the data, temporal features need to be extracted from the data which in this case is achieved by calculating a moving average (eq. 1) with a window of 5

$$MA(s_i, t, w) = \frac{1}{w} \sum_{j=t-w+1}^{t} s_{i,j}$$
 (1)

where s_i is a sensor reading and w is the window size, and calculating the gradient using the central difference at each time step (eq. 2)

$$g(i) = \frac{x(i+1) - x(i-1)}{2}$$

$$g(0) = x(1) - x(0)$$
(2)

where g(i) is the gradient index at i and x is the input data array. Data preprocessing steps also involve normalization and partitioning of the data into training, validation, and test sets. Finally, another random forest model is evaluated that

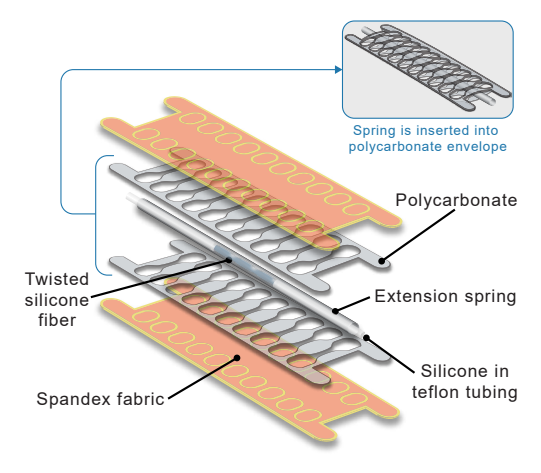


Fig. 3. Construction of a reconfigurable-chirality twisted beam with embedded twist sensor. The spring is inserted inside the polycarbonate skeleton causing it to distort and be under tension.

uses a time-lagged input (TL RF) from the raw sensor data

$$X = [x_1, x_2, \dots, x_N],$$
 where each $x_i \in \mathbb{R}^{15}$
 $x_i = [s_1(t_i), \dots, s_1(t_{i+4}), s_2(t_i), \dots, s_3(t_{i+4})]$

where each input feature vector X is a concatenation of 5 sequential data points from the three sensors. x_i is the i^{th} feature vector, comprised of sequential data points from sensors s1, s2, and s3.

2) Dynamic Chirality Sensing: A different approach is used to detect a beam's chirality in experiments with bistable reconfigurable twisted structures. Square cross-section silicone fiber waveguides of 3 cm length are created from silicone (Solaris, Smooth-On Inc) molded in a square glass capillary (Vitrocom, Inc., USA). These segments are pretwisted and inserted through a tube along the central axis of the beam. The pre-twisted fiber is fed by Solaris silicone in 2 mm diameter Teflon tubing. Further twisting decreases light transmission by causing light to encounter sidewalls at sharper angles than the critical angle for total internal reflection, while untwisting increases transmission. This feature is useful for monitoring bistable twisted structures, where the same limb can produce different foot motions depending on its chirality when oscillated at a constant frequency.

B. Experimental Setup

1) Single Beam Contact Test: This experiment follows the methodology used in [1] to show how the output trajectory of a soft twisted beam can be influenced by the driving frequency. The same hardware and experimental setup is used, with a 50 g weight. The beam is set to oscillate horizontally and the OptiTrak Prime optical motion tracking system captures the position data of the tip of the beam, which is then correlated with the OptiGap sensor readings. The main data outputs consist of x, y, z tip positions and three optical intensity readings at each sample point. These are recorded as the beam vibrates at frequencies ranging from 1 to 40 Hz.

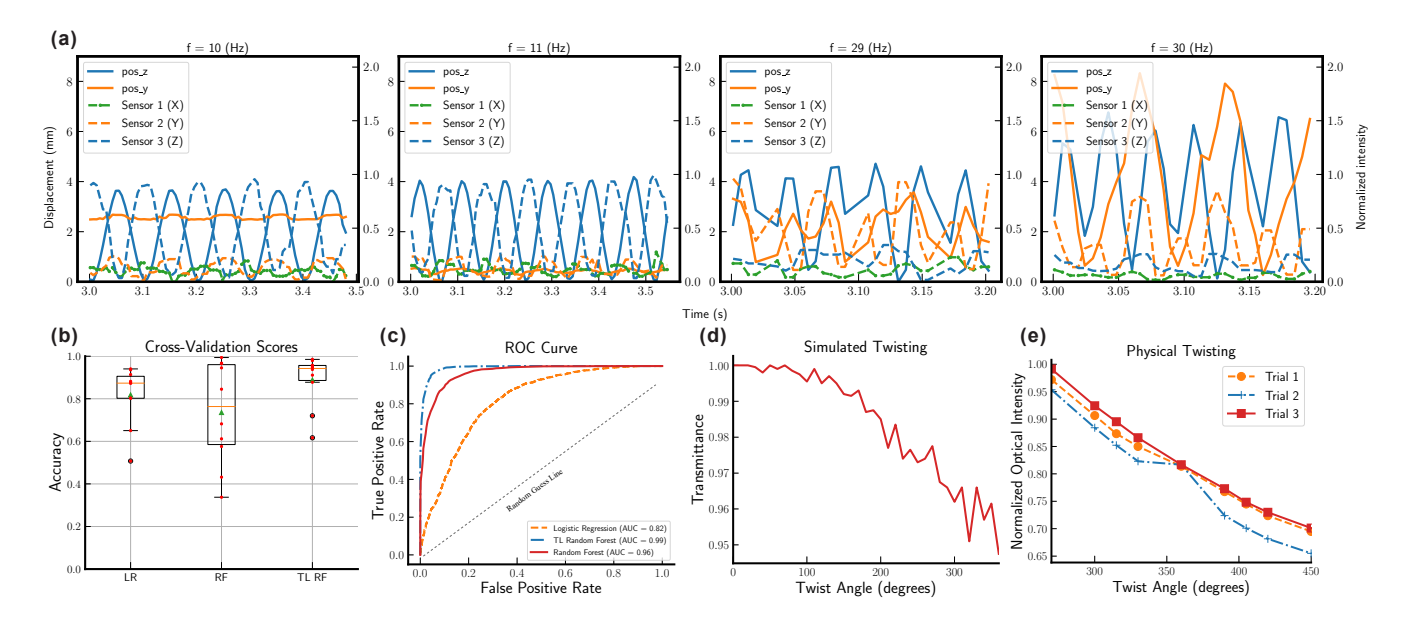


Fig. 4. Vibrating beam results: (a) The correlation between the position displacement and sensor intensity over 6 cycles at selected frequencies. (b) The 10-fold cross validation results show the TL random forest model as the best performer with a much tighter distribution than the rest. (c) The area under the curve (AUC) quantifies the models overall performance, with the TL random forest model showing the best performance of the three. Bistable twisted beam results: (d) COMSOL simulation results showing a reduction in optical transmittance as a square fiber is twisted. (e) Experimental results of twisting a square cross-section silicone fiber showing an attenuation of the signal with an increase in twist angle.

2) Bistable Twisted Limb and Gait Reconfiguration: The motivation behind using a bistable twisted limb is to explore gait reconfiguration. The limb, when oscillated horizontally at a constant frequency by a shaker, produces different foot motions depending on its chirality. This is captured by a camera and analyzed to understand the impact of chirality on the walking gaits of the robotic system.

III. RESULTS AND DISCUSSION

A. Vibrating Beam

The single beam contact test reveals distinct end-point trajectories at selected frequencies, as illustrated in Fig. 5, which mimic the trajectories presented in [1]. Arrows indicate the direction of motion at the contact point, providing insights into how the twisted beam interacts with the ground. This data is further substantiated by Fig. 6, which presents a Fourier transform analysis of the optical intensity readings from the OptiGap sensors. The dominant frequencies align well with the system input frequencies, validating the sensor's capability to accurately capture the vibrational characteristics of the twisted beams. This frequency analysis further supports the reliability of the OptiGap system in real-time sensing applications. Fig. 7 integrates the normalized optical intensities from the three OptiGap sensors with the endpoint trajectories at selected input frequencies.

The antagonistic placement of sensors 2 and 3 reveals insightful behavior of the beam's motion, offering a better understanding of how sensor placement can influence usefulness of the data. Fig. 4a presents a cycle analysis, plotting six cycles for the y and z positions, and normalized optical intensity. This figure reveals a strong correlation between each sensor's optical intensity and the beam's positional data,

TABLE I PERFORMANCE METRICS

Metric	Formula	
Accuracy	$\frac{TP + TN}{TP + TN + FP + FN}$	
Precision	$\frac{\text{TP}}{\text{TP} + \text{FP}}$	
Recall	$\frac{\text{TP}}{\text{TP} + \text{FN}}$	

providing a temporal dimension to the sensor's capabilities. This cycle analysis not only validates the sensor's real-time performance but also opens the door for advanced control algorithms that can adapt to dynamic changes in the robot's environment or operational parameters.

TABLE II
CLASSIFICATION RESULTS

Metric	Logistic Regression	Random Forest	TL Random Forest
Accuracy	75%	90%	95%
Precision	75%	90%	96%
Recall	74%	90%	95%

1) Binary Classification: The evaluation of the three models reveals varying levels of performance. The classification report in Table II indicates that the logistic regression model achieves an accuracy of 75%, precision of 75%, and recall of 74%. In contrast, the random forest model demonstrates an accuracy of 90%, precision of 90%, and recall of 90%. The TL RF model outperforms both, with an accuracy of 95%, precision of 96%, and recall of 95%. In a 10-fold cross-validation assessment shown in Fig. 4(b), the logistic regression model yields a mean accuracy of 81.82% with a standard deviation of 13.16%. The random forest model's mean accuracy stands at 73.56% with a standard deviation of

Contact Frequency Sweep Test: End Point Trajectory

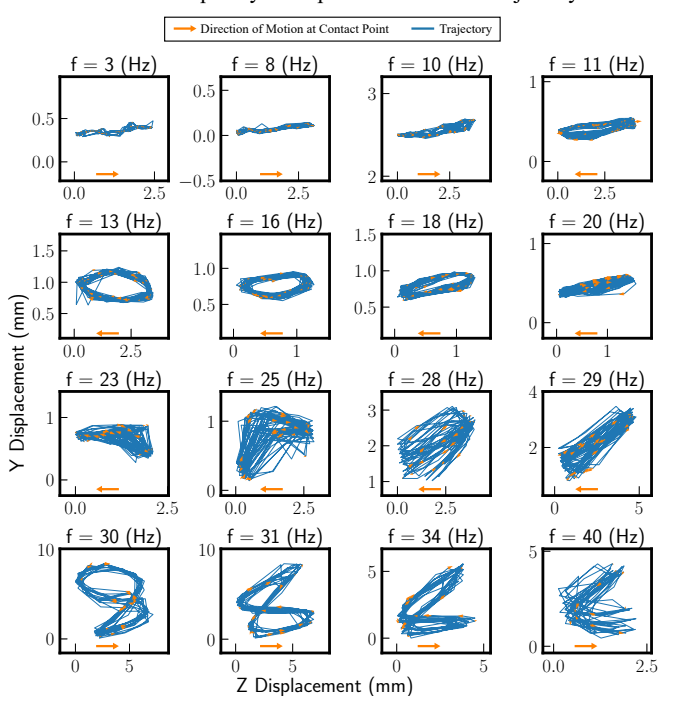


Fig. 5. **Single beam contact test results.** End point trajectories for selected frequencies with arrows showing the direction of motion at the contact point.

22.88%, while the TL RF model achieves a mean accuracy of 88.86% with a standard deviation of 11.63%. The ROC curve analysis in Fig. 4(c) further substantiates these findings, with the AUC values being 0.82 for logistic regression, 0.96 for random forest, and an impressive 0.99 for the TL RF model.

B. Embedded Chirality Sensing

Fig. 4d displays a COMSOL simulation of a square fiber subjected to twist, indicating a decrease in light transmittance with increasing twist angle. This data supports the underlying operational theory of the sensor. Fig. 4e provides experimental validation of the simulation, featuring a similar twisted fiber setup and its corresponding angle vs normalized optical intensity graph. Experimental data centered around a starting twist of 360° qualitatively confirms the simulation but has greater sensitivity to twisting than expected, possibly due to molding imperfections and elastic instabilitydriven wrinkling known to emerge during twisting of soft materials [32]. Fig. 8 demonstrates a practical application of the sensor, showing that a change in the chirality of a reconfigurable twisted beam results in a change in rotation direction. Taken together with earlier results, this confirms that a twisted waveguide threaded down the center of the beam can accurately provide information about its chirality and, consequently, the direction of motion.

C. Application

One application for both sensors aligns with the frequencycontrolled robot by Jiang et al. discussed earlier in this work [1]. These sensors can enable the robot to operate in

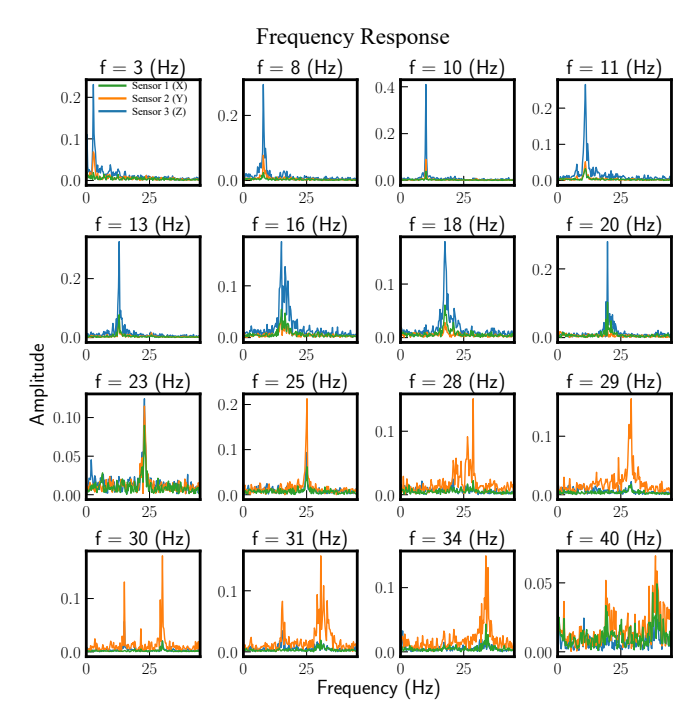


Fig. 6. **Frequency analysis.** Fourier transform of the optical intensity readings from the OptiGap sensors. The dominant frequencies match the system input frequencies, validating the sensor data.

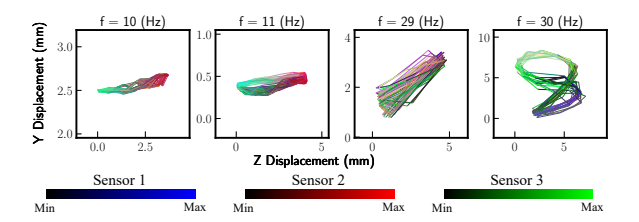


Fig. 7. **OptiGap sensor intensities.** The plot colors are composites based on the normalized intensity values from Sensor 1 (Blue), Sensor 2 (Red), and Sensor 3 (Green), especially showing the effects of the antagonistic placement of sensors 2 and 3.

both fixed and variable-frequency modes with programmable gaits and real-time feedback. In the variable-frequency mode, OptiGap can integrate into a control loop to ensure the desired motion direction is maintained, regardless of the surface's material characteristics, by monitoring each leg's contact direction. Conversely, in the fixed frequency mode, the legs' chirality can be dynamically altered, for instance, through temporary SMA actuation, thereby adjusting the robot's direction and monitored using the proposed internal chirality sensor.

IV. CONCLUSION

We successfully demonstrated and validated the OptiGap sensor's effectiveness in monitoring twisted beam dynamics while being mechanically transparent and leveraged basic machine learning techniques for distinguishing between forward and reverse gaits. The time-lagged random forest model excelled in binary classification, outperforming logistic regression (which struggled with the non-linearity of the data),

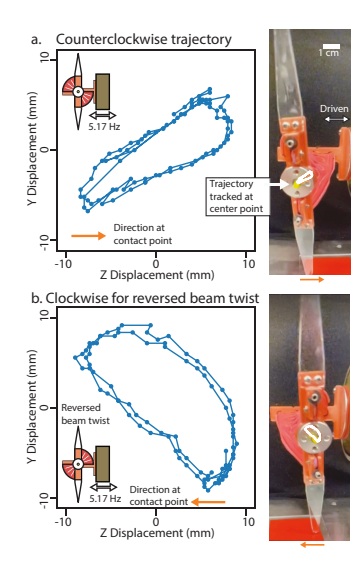


Fig. 8. **Bistable twisted beam trajectories.** The direction of motion of the twisted limb (a,b) reverses when the chirality is flipped. The reversal of the trajectory results in a change of direction at the contact point with the ground.

and standard random forest model (which exhibited potential over-fitting). The pre-twisted waveguide results confirm the effectiveness of soft optical sensors in detecting beam chirality. The experimental data validate the sensor's capability to capture variations in light transmittance with respect to twist angle, for a lightweight and flexible means of monitoring the state of twisted beams in reconfigurable systems.

REFERENCES

- [1] Y. Jiang, F. Chen, and D. M. Aukes, "Tunable dynamic walking via soft twisted beam vibration," *IEEE robotics and automation letters*, vol. 8, pp. 1967–1974, Apr. 2023.
- [2] P. Bupe and C. K. Harnett, "OptiGap: A modular optical sensor system for bend localization," in 2023 IEEE International Conference on Robotics and Automation (ICRA), pp. 620–626, May 2023.
- [3] Y. Jiang, M. Sharifzadeh, and D. M. Aukes, "Reconfigurable soft flexure hinges via pinched tubes," in 2020 IEEE/RSJ International Conference on Intelligent Robots and Systems (IROS), pp. 8843–8850, ieeexplore.ieee.org, Oct. 2020.
- [4] M. Jiang, Q. Yu, and N. Gravish, "Vacuum induced tube pinching enables reconfigurable flexure joints with controllable bend axis and stiffness," in 2021 IEEE 4th International Conference on Soft Robotics (RoboSoft), pp. 315–320, Apr. 2021.
- [5] Y. Jiang, M. Sharifzadeh, and D. M. Aukes, "Shape change propagation through soft curved materials for Dynamically-Tuned paddling robots," in 2021 IEEE 4th International Conference on Soft Robotics (RoboSoft), pp. 230–237, Apr. 2021.
- [6] M. Sharifzadeh and D. M. Aukes, "Curvature-Induced buckling for Flapping-Wing vehicles," *IEEE/ASME Transactions on Mechatronics*, vol. 26, pp. 503–514, Feb. 2021.
- [7] P. Bupe, D. J. Jackson, and C. K. Harnett, "Electronically reconfigurable virtual joints by shape memory Alloy-Induced buckling of curved sheets," in *SoutheastCon* 2022, pp. 598–604, Mar. 2022.
- [8] H. X. Tan, N. N. Aung, J. Tian, M. C. H. Chua, and Y. O. Yang, "Time series classification using a modified LSTM approach from accelerometer-based data: A comparative study for gait cycle detection," *Gait & posture*, vol. 74, pp. 128–134, Oct. 2019.
- [9] H. T. T. Vu, F. Gomez, P. Cherelle, D. Lefeber, A. Nowé, and B. Vanderborght, "ED-FNN: A new deep learning algorithm to detect percentage of the gait cycle for powered prostheses," *Sensors*, vol. 18, July 2018.
- [10] S. Khandelwal and N. Wickström, "Novel methodology for estimating initial contact events from accelerometers positioned at different body locations," *Gait & posture*, vol. 59, pp. 278–285, Jan. 2018.

- [11] D. Zeng, C. Qu, T. Ma, S. Qu, P. Yin, N. Zhao, and Y. Xia, "Research on a gait detection system and recognition algorithm for lower limb exoskeleton robot," *Journal of the Brazilian Society of Mechanical Sciences and Engineering*, vol. 43, p. 298, May 2021.
- [12] B. Su, C. Smith, and E. Gutierrez Farewik, "Gait phase recognition using deep convolutional neural network with inertial measurement units," *Biosensors*, vol. 10, Aug. 2020.
- [13] B. Chakraborty, "A proposal for classification of multisensor time series data based on time delay embedding," *International Journal* on Smart Sensing and Intelligent Systems, vol. 7, pp. 1–5, Jan. 2014.
- [14] T. Hastie, R. Tibshirani, and J. Friedman, The Elements of Statistical Learning. Springer New York.
- [15] K. Kirasich, T. Smith, and B. Sadler, "Random forest vs logistic regression: Binary classification for heterogeneous datasets," SMU Data Science Review, vol. 1, no. 3, p. 9, 2018.
- Data Science Review, vol. 1, no. 3, p. 9, 2018.
 [16] V. Bahel, S. Pillai, and M. Malhotra, "A comparative study on various binary classification algorithms and their improved variant for optimal performance," in 2020 IEEE Region 10 Symposium (TENSYMP), pp. 495–498, June 2020.
- [17] G. Olson and Y. Mengüç, "Helically wound soft actuators for torsion control," in 2018 IEEE International Conference on Soft Robotics (RoboSoft), pp. 214–221, ieeexplore.ieee.org, Apr. 2018.
- [18] S. Armon, E. Efrati, R. Kupferman, and E. Sharon, "Geometry and mechanics in the opening of chiral seed pods," *Science*, vol. 333, pp. 1726–1730, Sept. 2011.
- [19] J. Choi, S. H. Ahn, and K.-J. Cho, "Design of fully soft actuator with Double-Helix tendon routing path for twisting motion," in 2020 IEEE/RSJ International Conference on Intelligent Robots and Systems (IROS), pp. 8661–8666, ieeexplore.ieee.org, Oct. 2020.
- [20] Y. Zhao, Y. Chi, Y. Hong, Y. Li, S. Yang, and J. Yin, "Twisting for soft intelligent autonomous robot in unstructured environments," *Proc. Natl. Acad. Sci. U. S. A.*, vol. 119, p. e2200265119, May 2022.
- [21] J.-E. Shim, Y.-J. Quan, W. Wang, H. Rodrigue, S.-H. Song, and S.-H. Ahn, "A smart soft actuator using a single shape memory alloy for twisting actuation," *Smart Mater. Struct.*, vol. 24, p. 125033, Nov. 2015.
- [22] A. F. Arrieta, V. Van Gemmeren, A. J. Anderson, and P. M. Weaver, "Dynamics and control of twisting bi-stable structures," *Smart Mater. Struct.*, vol. 27, no. 2, p. 025006, 2018.
- [23] H. Zhao, K. O'Brien, S. Li, and R. F. Shepherd, "Optoelectronically innervated soft prosthetic hand via stretchable optical waveguides," *Science Robotics*, vol. 1, Dec. 2016.
- [24] S. Sareh, Y. Noh, M. Li, T. Ranzani, H. Liu, and K. Althoefer, "Macrobend optical sensing for pose measurement in soft robot arms," *Smart Materials and Structures*, vol. 24, p. 125024, Nov. 2015.
- [25] M. McCandless, F. J. Wise, and S. Russo, "A Soft Robot with Three Dimensional Shape Sensing and Contact Recognition Multi-Modal Sensing via Tunable Soft Optical Sensors," in 2023 IEEE International Conference on Robotics and Automation (ICRA), May 2023.
- [26] H. A. Wurdemann, S. Sareh, A. Shafti, Y. Noh, A. Faragasso, D. S. Chathuranga, H. Liu, S. Hirai, and K. Althoefer, "Embedded electro-conductive yarn for shape sensing of soft robotic manipulators," in 2015 37th Annual International Conference of the IEEE Engineering in Medicine and Biology Society (EMBC), 2015.
- [27] J. Avery, M. Runciman, A. Darzi, and G. P. Mylonas, "Shape Sensing of Variable Stiffness Soft Robots using Electrical Impedance Tomography," in 2019 International Conference on Robotics and Automation (ICRA), 2019.
- [28] F. Al Jaber and K. Althoefer, "Towards creating a flexible shape senor for soft robots," in 2018 IEEE International Conference on Soft Robotics (RoboSoft), 2018.
- [29] G. Rizzello, P. Serafino, D. Naso, and S. Seelecke, "Towards Sensorless Soft Robotics: Self-Sensing Stiffness Control of Dielectric Elastomer Actuators," *IEEE Transactions on Robotics*, vol. 36, no. 1, pp. 174–188, 2020.
- [30] K. C. Galloway, Y. Chen, E. Templeton, B. Rife, I. S. Godage, and E. J. Barth, "Fiber Optic Shape Sensing for Soft Robotics," *Soft Robotics*, vol. 6, pp. 671–684, Oct. 2019.
- [31] H. Jo, Y. Bae, Y. Song, J. Han, and J.-H. Song, "Stretchable multi-mode sensor with single and simultaneous sensing modes for human neck motion tracking," *Applied Materials Today*, vol. 33, p. 101874, Aug. 2023.
- [32] P. Ciarletta and M. Destrade, "Torsion instability of soft solid cylinders," IMA J Appl Math, vol. 79, pp. 804–819, Jan. 2014.